ORIGINAL RESEARCH PAPER

Improvement of mechanical properties of gas tungsten arc and electron beam welded AA2219 (Al–6 wt-%Cu) alloy

Biju S. Nair*[1], G. Phanikumar[2], K. Prasad Rao[2] and P. P. Sinha[1]

Despite its excellent weldability characteristics, AA2219 suffers from poor fusion zone strength under the as welded condition. In the present work, it is attempted to increase the mechanical properties of the as welded fusion zone of this alloy by increasing the weld cooling rates and multipass welding. The cooling rate was increased with the use of high intense heat source, namely electron beam in a pulsed current mode. Multipass gas tungsten arc welding was carried out using direct current straight polarity. These techniques resulted in a significant improvement in fusion zone hardness and tensile properties, which is attributed to reduced copper segregation and natural aging as well as aging caused by heat of multipass welding.

Keywords: AA2219, Pulsed electron beam welding, Gas tungsten arc welding, Multipass, Mechanical properties

Introduction

Aluminium–copper alloy AA2219 (Table 1) is an age hardenable alloy considered for aerospace applications. Unlike its other age hardenable alloy counterparts such as 6000 (Al–Si–Mg) and 7000 (Al–Zn–Mg) series, AA2219 exhibits excellent weldability characteristics. Though the alloy has got an edge over its 6000 and 7000 series counterparts in terms of weldability, it suffers from poor as welded joint strength. For example, when welded using a filler wire (Table 1), the fusion zone exhibits a yield strength (YS) of $\sim$140 MPa and a ultimate tensile strength (UTS) of 250 MPa as against the strengths of the corresponding base metal of 370 and 470 MPa. If the strength of the fusion zone can be increased to any degree, the cost and weight saving would be significant.

The loss of strength is due to the melting and quick resolidification, which renders all the strengthening precipitates to dissolve. Earlier studies[1] have shown that copper segregation in the as weld structure is the main reason, because of which the fusion zone does not respond to natural aging. These studies suggested that any attempt to decrease the copper segregation by methods such as high weld cooling rates as obtained in electron beam welding (EBW) and weld pool agitation which could be obtained by pulsed current techniques[2] will be helpful. It is expected that such lower copper segregation will make availability of copper in solution, which makes the fusion zone respond to natural aging. High cooling rates may also aid in reducing the grain size that may be helpful in improving the ductility of weld joint.

In the case of aluminium alloys, current pulsing was used for fusion zone grain refinement in gas tungsten arc welding (GTAW).[3–5] Previous studies with scandium addition[6] showed grain refinement and increased tensile strength in AA2219 alloy welds. Madhusudhan Reddy *et al.*[7,8] have reported a significant refinement of fusion zone solidification structure and a reduction in segregation, leading to a substantial improvement in solidification cracking resistance and weld tensile properties in type 1441 Al–Li alloy when welded using a pulsed alternating current. These welding techniques resulted in a substantial grain refinement and an increase in yield strength of the weld metal. It has also been reported that a further increase in the yield stress could be obtained by simultaneous application of pulsing and arc oscillation. Janaki Ram *et al.*[5] have also reported a significant grain refinement and an improvement in the tensile properties in AA2090 (Al–Li) alloy and type AFNOR 7020 (Al–Zn–Mg) alloy welds using current pulsing. It would also be interesting to apply multipass GTAW technique with the pulsed current as it is expected to cause the aging of underlying passes and improve the fusion zone strength. Pulsing in welding is known to have an effect on the periodic variation in arc force, enhancing the weld pool turbulence and lowering the temperature gradient and peak temperature in the weld zone.[7] Not many reports are available as for the effects of multipass welding on mechanical properties of AA2219 welds.

It is well known that the EBWs of most of the weldable materials including aluminium alloys exhibit superior mechanical properties to the welds made using GTAW technique. Extensive work on the optimisation of parameters and evaluation of mechanical properties was performed on EBWs of AA2219 alloy.[9,10] Comparison of mechanical properties reported in

[1]Mechanical Engineering Entity, Vikram Sarabhai Space Center, Thiruvananthapuram, Kerala 695022, India
[2]Department of Metallurgical and Materials Engineering, Indian Institute of Technology Madras, Chennai 600036, India

*Corresponding author, email s_biju@vssc.gov.in

Published by Maney on behalf of the Institute
Received 9 March 2007; accepted 9 July 2007
DOI 10.1179/174329307X227210

literature[11,12] shows that the difference in the values of tensile and proof strength between EBWs and GTAWs or variable polarity plasma arc welds was $\sim$100 MPa, particularly in the case of thicker sections. It would be worthwhile to study the effects of the application of EBW with the pulsed current on the mechanical properties of AA2219 as it is expected to result in higher weld cooling rates and reduced copper segregation compared to their continuous current counterparts.

Therefore, in the present work the approach adopted was to increase the weld cooling rates by GTAW and EBW techniques. These approaches were to apply multipass GTAW with direct current straight polarity in continuous and pulsed modes, and EBW with a pulsed current mode. In the case of GTAW, cooling rates were further increased by heat extraction using a copper back-up. The mechanical properties were compared with those of the similar welds made using a stainless steel back-up.

Experimental details

AA2219 alloys with dimensions of $400 \times 60 \times 7{\cdot}2$ and $250 \times 60 \times 7{\cdot}2$ mm were taken for GTAW and EBW respectively. The initial base metal was solution heat treated, 8% cold worked and precipitation hardened at 163°C for 24 h. Before welding, stripping of the milled joint envelope was carried out with a scraping tool. In the case of multipass GTAW, stainless steel wire brushing followed by vacuum suction was used to keep the sample clean.

Automatic GTAW was performed with a direct current and straight polarity on V joint with 60° groove angle without root gap. Weld current was applied in both continuous and pulsed modes. Welding was performed on workpieces using two types of back-up plates, namely stainless steel and copper (the results presented in section 'Results' pertain to welds with copper back-up). A $\phi 1{\cdot}6$ mm wire of near base metal composition (Table 1) was used as the filler material. High purity helium was used for shielding the weld pool. Welding was carried out in single pass, two passes, three passes and four passes on separate workpieces. About 75% volume filling was achieved during the first pass. The heat input applied during the first pass was $\sim 1{\cdot}5$ times (1·15 kJ mm^{-1}) more than that of the succeeding weld runs (second, third and fourth passes). Electron beam welding was carried out with square butt joint in both continuous current mode and pulsed current mode, where pulsing was achieved by switching between on and off at a given frequency. The chamber vacuum was maintained at $<3 \times 10^{-4}$ mbar. Electron beam welds with a continuous current were made with a heat input of 190 J mm^{-1} whereas 156 J mm^{-1} was only applied in the pulsed mode.

X-ray radiography was carried out to evaluate the weld integrity. Scanning electron microscope (SEM) with energy dispersive X-ray (EDS) analysis was used for studying the variation of solute content (copper) across the grains. Transmission electron microscopy (TEM) was used on samples taken from the single pass fusion zone and the first pass of multipass welds to observe the absence or presence of strengthening precipitates. Microhardness survey was carried out with a 100 mg load. Transverse tensile test was performed as per ASTM E 8M. Three specimens were tested to arrive at an average value for each category.

Table 1 Chemical composition of AA2219 base alloy and ER2319 filler, wt-%

Alloy	Cu	Mn	Zr	V	Ti	Fe	Si	Al
AA2219	5·95	0·27	0·10	0·09	0·06	0·10	0·05	Bal.
ER2319	6·10	0·29	0·15	0·10	0·15	0·10	0·04	Bal.

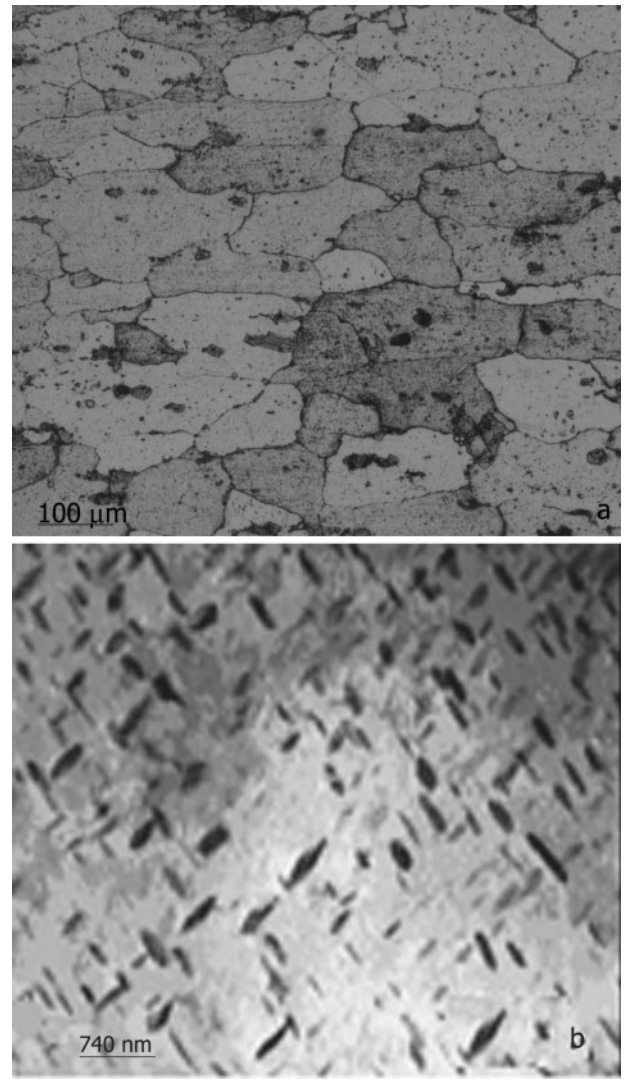

1 *a* Base alloy-optical micrograph and *b* Base alloy-Transmission electron micrograph

Results

Microstructural aspects

Base metal AA2219

Under the as received condition, the optical microstructure of AA2219 aluminium alloy, taken along the cross-section of the base metal, revealed round particles distributed in the interior of matrix (Fig. 1*a*). Needle shaped precipitates were found distributed homogeneously within the grain (Fig. 1*b*), the microanalysis of which conformed to the composition of $CuAl_2$.

Multipass GTAWs

X-ray radiographic test did not reveal the entrapment of aluminium oxide in the weld fusion zone. Figure 2*a*

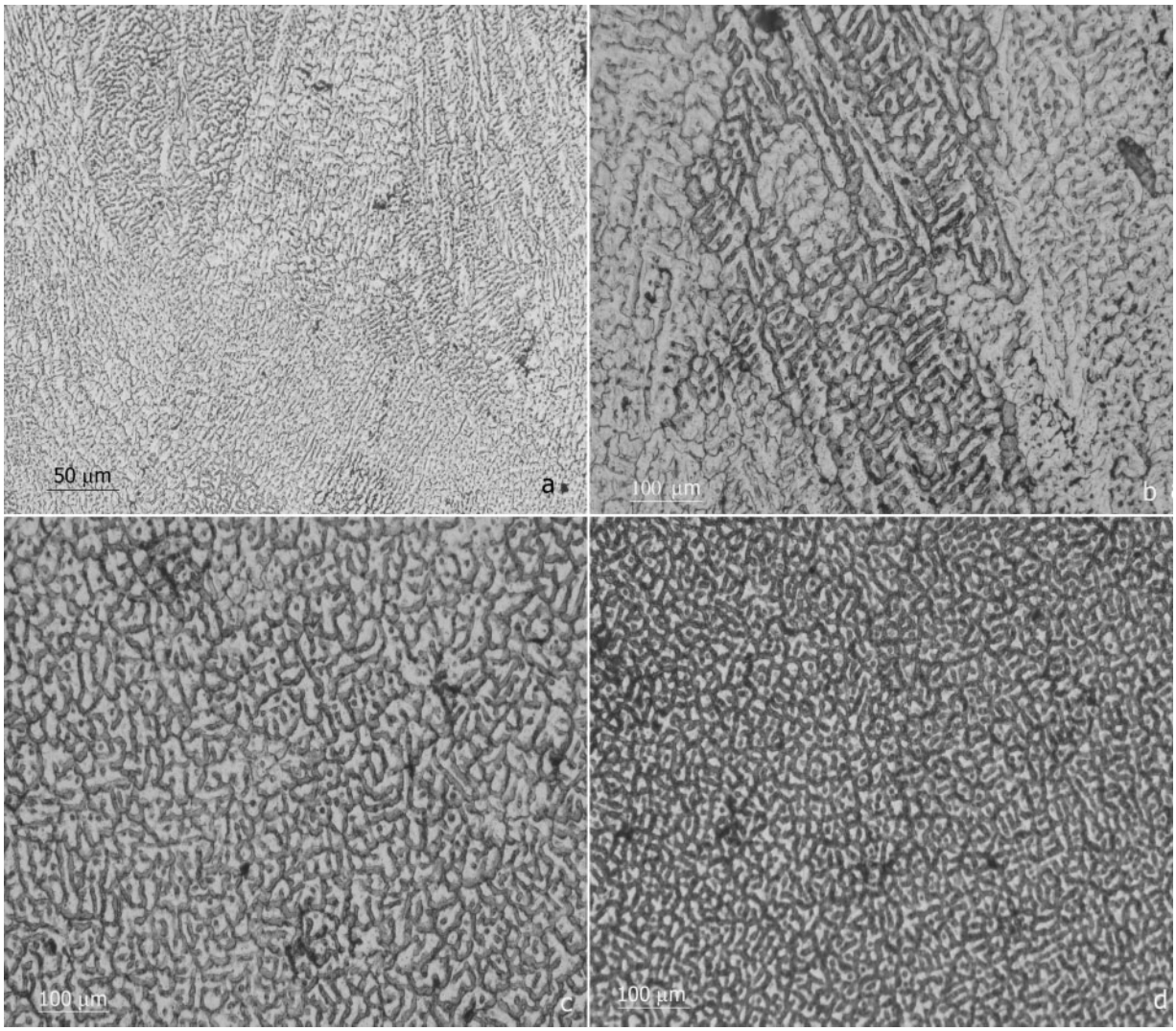

b first pass; *c* second pass; *d* fourth pass

2 *a* micrograph showing interface between gas tungsten arc welding passes *b–d* dendritic size and spacing in specimen with copper back-up-continuous current, four-pass weld

shows the micrograph of the etched structure of multipass welds. In the first pass (Fig. 2*b*), dendritic spacing was found moderately larger. This is attributed to the relatively larger heat input applied for that weld run. The dendritic spacing was gradually reduced in the second, third and fourth passes (Fig. 2*c* and *d*), which can be attributed to the relatively lower heat input applied for these weld runs.

Secondary electron images of the fusion zone with copper and stainless steel back-up (Fig. 3*a–c*) show the eutectic morphology. The results showed that the heat input, back-up material and current pulsing affected its size and distribution. Eutectic morphology was found coarser and continuous when welded with a continuous current and a stainless steel back-up (Fig. 3*a*). When a copper back-up was used under the same weld conditions, significantly finer and discontinuous eutectics were only seen (Fig. 3*b*). With multipass welding, presumably due to the reheating effect, interdendritic and grain boundary segregation in the first pass (Fig. 3*c*) became finer and discontinuous.

The TEM images for the GTAWs fusion zone specimen are shown in Figs. 4 and 5. As mentioned earlier, samples were taken from the single pass fusion zone and the first pass of multipass welds. Single pass welded fusion zone was found to be free of precipitate (Fig. 4). In multipass welds, thin disc type strengthening precipitates ($\sim$500 nm long and 40 nm thick) were noticed in the first pass (Fig. 5*a–d*). With a pulsed current, the precipitates were finer and their regeneration was more pronounced (Fig. 5*b*) than continuous current welds (Fig. 5*a*). The restoration was found to enhance with an increase in the number of passes (Fig. 5*c* and *d*). Microanalysis of these precipitates confirmed the $CuAl_2$ intermetallic. The emergence of these precipitates could be attributed to the solute saturation within primary dendrites, natural aging and the aging effect caused by subsequent passes.

Electron beam welds

Electron beam weld fusion zone was found relatively smaller than that of the GTAWs. When pulsed, the EBWs fusion zone is narrower and V shaped. Figure 5 shows the secondary electron image of fusion zone microstructure of EBWs, indicating the eutectic morphology. The weld with the continuous current showed relatively coarser eutectic distribution than the one with the pulsed current (Fig. 6*a*). Electron beam weld

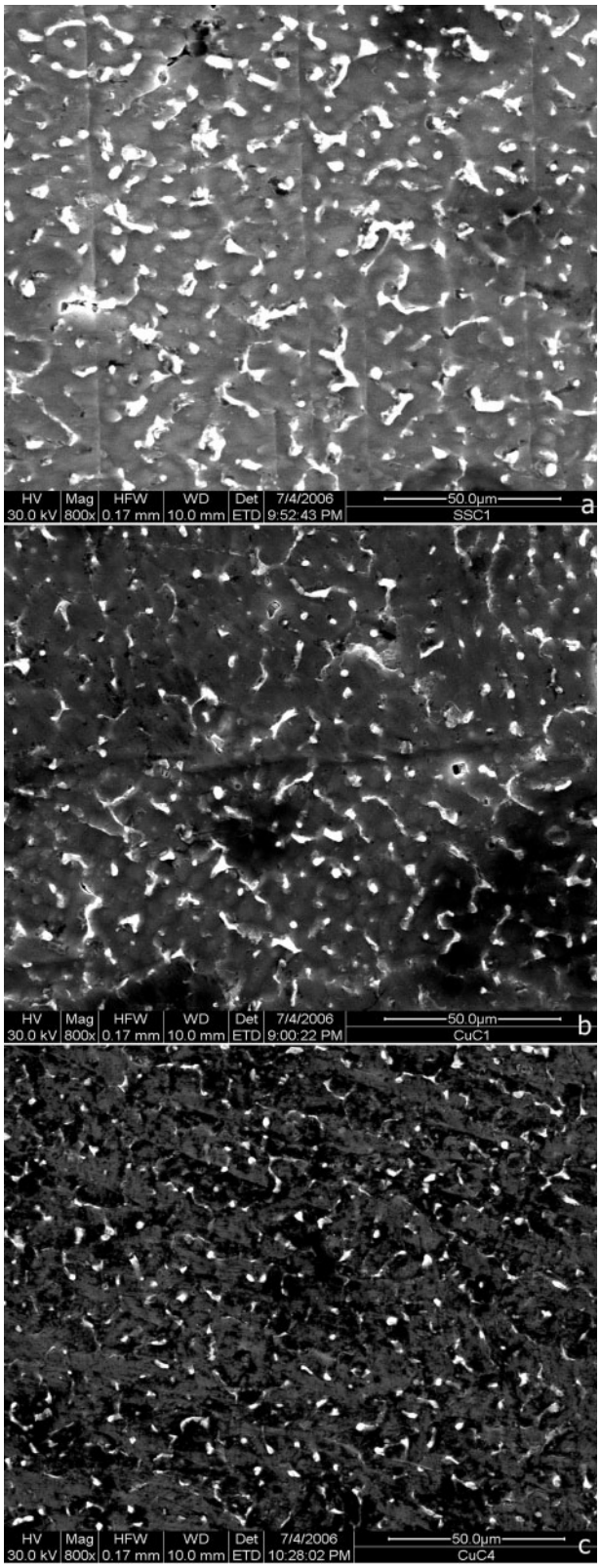

a single pass with stainless steel back-up; *b* single pass with copper back-up; *c* first pass of four pass weld with copper back-up

3 Image (SEM) of fusion zone of GTAWs

with the pulsed current showed the finest eutectic morphology among the entire weld samples (Fig. 6*b*). This is mainly due to the very high solidification rates associated with such welding. Because of the prior thermal condition and faster processing, more dislocations were found in the as welded fusion zone.

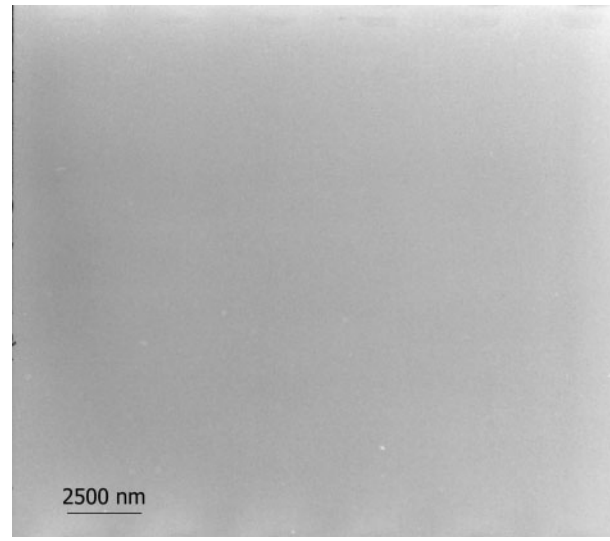

4 Transmission electron micrograph: Continuous current, single pass gas tungsten arc weld

Microanalysis

A peak in a microanalysis line scan plot is indicative of a solute segregated region. Cross-sectional line scan indicated copper segregation in the fusion zone, which was found to be relatively more with continuous current single pass GTAWs with a stainless steel back-up. Its severity could be reduced when the back-up was replaced with copper of the same size and further reduced with overlay weld passes. Compared to all the specimens, copper segregation was minimal in the case of electron beam pulsed welds. Average values of solute partitioning inside the grain and at the grain boundary are shown in Table 2 for different samples. The grain boundary particles in these welds are mainly Al–Cu eutectic phase which contains ~26 wt-%Cu for GTAWs with a stainless steel back-up. With the copper back-up and an increase in the number of passes, the grain boundary copper segregation decreased. Such segregation was more pronounced in the case of GTAWs than that in EBWs. In the latter case, copper distribution is relatively more uniform throughout the matrix.

Mechanical properties

Table 3 shows the average hardness around the centre of as welded fusion zone. Measurements were taken on transverse cross-section at 3 mm distance from the base of specimens. In multipass welding, hardness of the first pass was found to increase with the number of subsequent weld runs. Hardening effect was more noticeable with a pulsed current than that with a continuous current. The hardness of EBWs was found relatively higher than that of GTAWs. Table 4 shows the values of tensile strength for the fusion zone. The values of YS and UTS represent the strength of fusion zone only, as all the transverse tensile specimens failed in the fusion zone. Base alloy strength is shown for comparison.

Table 2 Local composition measured using SEM and EDS, wt-%Cu

	SSC1	CuC1	CuC4	EB1
Grain	6·63	4·45	3·88	4·45
Grain boundary	25·80	21·38	16·71	7·44

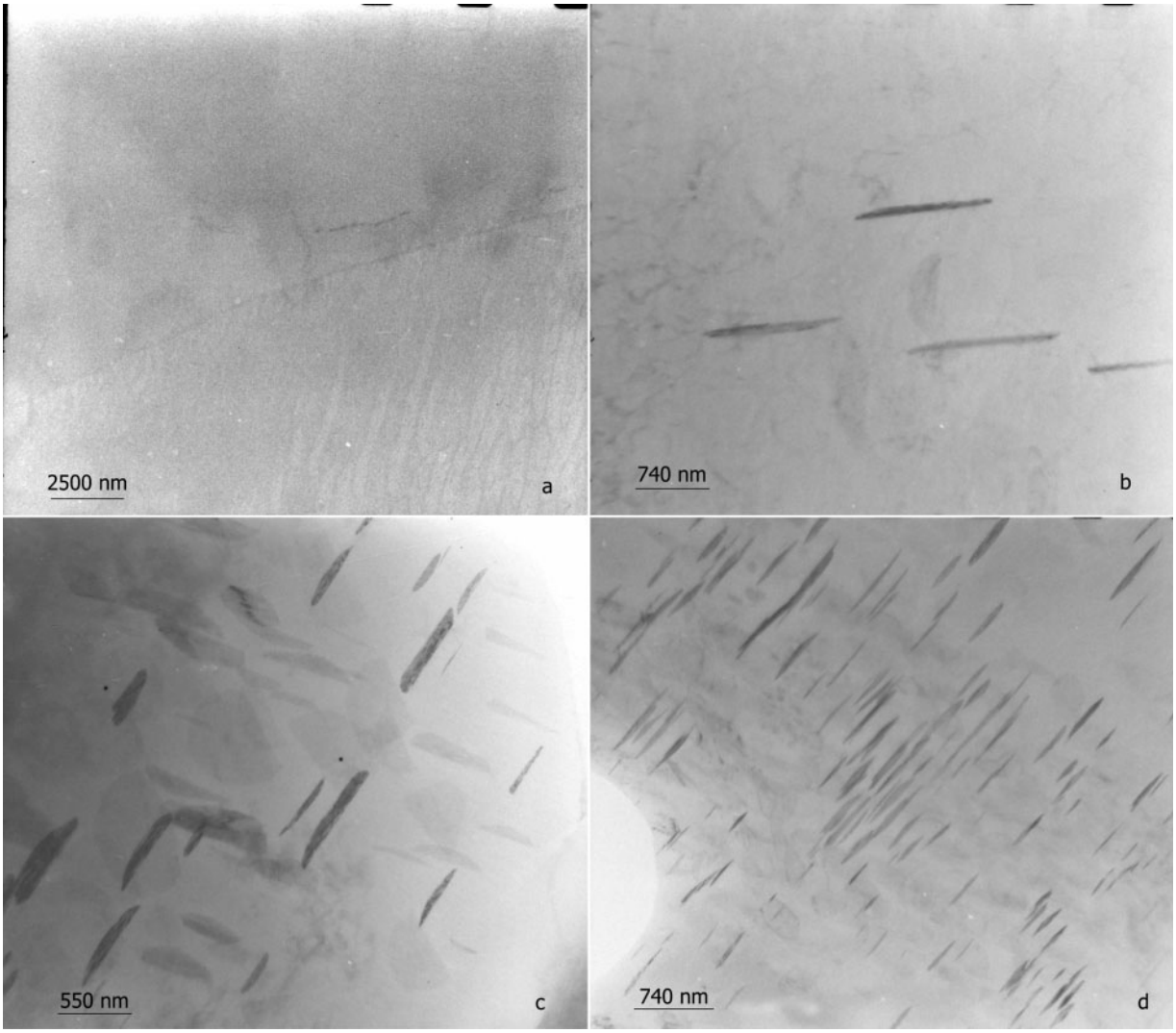

a continuous current, two pass; *b* pulsed current, two pass; *c* continuous current, four pass; *d* pulsed current, four pass

5 Transmission electron micrograph: First pass of multipass gas tungsten arc welds

Multipass welds with a copper back-up showed higher YS values than their counterpart with a stainless steel back-up (Table 4). Electron beam welded specimens showed the highest strength values. Values of YS and UTS of EBWs were almost the double of the GTAWs with a stainless steel back-up.

Discussion

Multipass GTAWs

Compared to single pass welding, multipass welding demands lower heat input, which reduced overall weld zone grain size and dendritic size. Interdendritic segregation was found to diminish towards the first weld pass, which is attributed to the reheating induced microstructural modification. Shelyagin *et al.*[13] did experiments on thick steel plates by laser and laser arc hybrid welding and concluded that in multipass welding, subsequent metal layers provide heat treatment of the previously deposited ones and optimal conditions are created for cooling of the weld bead. Although there is distinction with welding of steel, in aluminium alloys the

Table 3 Comparison of microhardness in fusion zone of GTAWs with copper back-up and EBWs

Category of weld	Mode	No. of weld run	Hardness, HV
GTAW	C*	1	86
GTAW	C*	2	85
GTAW	C*	3	90
GTAW	C*	4	100
GTAW	P†	1	87
GTAW	P†	2	86
GTAW	P†	3	96
GTAW	P†	4	102
EBW	C*	1	102
EBW	P†	1	110

Continuous weld.
†Pulsed weld.

Table 4 Tensile strength of GTAWs and EBWs

Category of weld with back-up	Mode	No. of weld run	UTS, MPa	YS, MPa
GTAW-SS*	C	1	246	133
GTAW-SS*	C	4	273	142
GTAW-Cu†	C	1	262	143
GTAW-Cu†	C	4	284	189
GTAW-SS*	P	1	249	136
GTAW-SS*	P	4	283	154
GTAW-Cu†	P	1	271	167
GTAW-Cu†	P	4	288	220
EBW	C	1	328	256
EBW	P	1	325	274
Base alloy	T87	–	464	366

*Stainless steel back-up.
†Copper back-up.

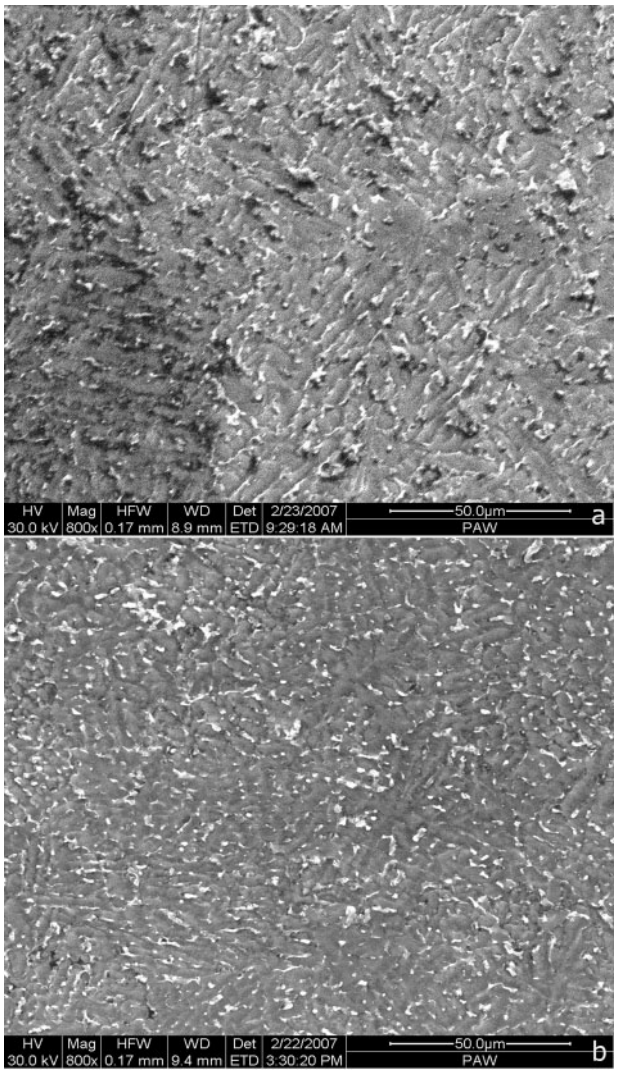

6 Scanning electron image: Fusion zone of electron beam welds *a* continudus current *b* pulsed current

effect of thermal cycling on the prior welded zone is found to favourably transform the as cast microstructure. Earlier studies[14] on 7·4 mm thick AA2219 in a continuous mode showed a lower toughness at fusion boundary and crack propagation along the brittle interconnected solute network in that region leading to failure. The present study using multipass resulted in more interfaces within the weld zone and made the fusion boundary tortuous. Tensile failure could be shifted from fusion boundary to fusion zone, which took place at higher loads than single pass welds. Earlier studies by Van Boggler *et al.*[15] showed the effect of coarsening and rounding off of grains through mechanisms such as levelling of concentration gradient and reduction in surface energy when exposed to relatively longer isothermal holding and low cooling rates. By allowing reheating as in multipass welding, the columnar dendritic structure in the exposed weld zone was favourably modified.

Earlier studies showed that the weld metal strength will depend on the solute supersaturation, which determines the subsequent aging response and YS.[16] The usage of a copper back-up in lieu of stainless steel resulted in finer and discontinuous eutectics. This could be attributed to the higher cooling rates experienced by the weld with a copper back-up. As a consequence of multipass welding, a considerable reduction in volume fraction of eutectics in terms of both size and composition has been achieved. Interconnected eutectic network available in single pass fusion welds was fragmented and redistributed. It is observed from the cross-sectional microanalysis that as a result of multipass welding, there is a considerable reduction in the solute segregation. This means that the solute level within the grain of multipass fusion zone is higher than that of the single pass welds. Such solute saturation favoured precipitation and strength.

Studies carried out by Hartman *et al.*[12] using variable polarity plasma arc welding showed that the flow stress increases with number of weld runs without an appreciable change in the ultimate strength. Apart from the effect of heat input on dendritic spacing, because of reheating, underlying passes are expected to partially restore strengthening precipitates. Time–temperature reaction due to thermal recycling, copper back-up and interpass holding resulted in the diffusion of a few strengthening precipitates and its strength was found to increase in proportion to the number of weld passes. The gain of $\sim$15 HV over single pass weld measures extra strength imparted as a consequence of solute redistribution in the root because of thermal cycling, precipitate regeneration and natural aging.

Multipass welding in the pulsed mode has shown a considerable increase in hardness and strength. Because of reduced heat input and modified convectional forces, pulsing is favourable for fine grained microstructure. Precipitate reappearance from the second weld run onwards was evidenced with pulsed energy. As fusion zone grains were more refined because of weld pool turbulence and reduced peak temperature, *in situ* aging response of pulsed gas tungsten arc was better.

Electron beam welds

Higher processing speed in EBW causes rapid melting and solidification, because of which the width of the fusion zone is small. As a result of high cooling rates, complete dissolution of precipitates is unlikely. Earlier studies[1] showed availability of fine round precipitates throughout EBWs fusion zone. Vaithyanathan *et al.*[17] have discussed about the formation of fine round precipitates in Al–Cu alloy system during the early stage of precipitation.

In EBW, the partition coefficient is closer to unity indicating minimum segregation at gain boundaries. Highly dislocated matrix and uniform distribution of Cu will enable natural aging. Koteswara Rao *et al.*[1] reported even distribution of copper in continuous current EBWs of AA2219. The present study using SEM images and microanalysis showed reduced solute segregation within the fusion zone. Fine grained microstructure, relatively larger number of dislocations in the fusion zone, reduced copper segregation, solute supersaturation, few microporosities and the presence of strengthening precipitates in the fusion zone of EBWs could be the major reasons for the higher fusion zone strength. Higher strength of electron beam pulsed weld over continuous could be due to lower heat input that further reduced solute segregation and grain size, favoured survival of more dislocations and precipitates.

The study showed that an improvement in mechanical properties of GTAWs close to that of EBWs is possible

through optimisation of weld sequencing in multipass mode with a copper back-up.

Conclusions

1. Direct current straight polarity GTAW, under helium environment, was found to deliver strong AA2219 weld joints.

2. Compared to single pass continuous current GTAW, multipass with optimised energy input, copper back-up and interpass dwell provided microstructural modifications within the fusion zone. This resulted in lowering solute segregation, precipitate regeneration by aging and fusion line strengthening. These factors contributed to the enhanced strength of multipass welds. Application of pulsed current further improved the mechanical properties.

3. Higher processing rate and vacuum environment are the key contributors for the additional strength of EBWs. A considerable reduction in heat input was achieved with pulsed EBW. Compared to continuous current, pulsed EBW technique resulted in higher fusion zone hardness and strength because of fine grains, lowest copper segregation, more dislocations, precipitate survival and natural aging.

4. The fusion zone YS of 220 MPa and the UTS of 288 MPa were achieved by pulsed GTAW. The corresponding values by pulsed EBW were 274 and 325 MPa.

Acknowledgement

Authors thanks Mr. G. Kothandaraman & Mr. S. Rakesh of Vikram Sarabhai Space Centre for their support & encourangement.

References

1. S. R. Koteswar Rao, K. Sreenivasa Rao, G. Madhusudhan Reddy, M. Kamaraj and K. Prasad Rao: *Mater. Charact.*, 2005, **55**, 345–354.
2. S. R. Koteswar Rao, G. Madhusudhan Reddy, M. Kamaraj and K. Prasad Rao: *Mater. Sci. Eng. A*, 2005, **A404**, 227–234.
3. J. G. Garland: *Mater. Trans.*, 1991, **32**, 145–150.
4. F. Matsuda, M. Ushio, K. Nakata, K. Tsukamoto and Y. Miyanaga: *Trans. Jpn. Weld. Res. Inst.*, 1978, **7**, (2), 139–141.
5. G. D. Janaki Ram, R. Murugesan and S. Sundaresan: *Pract. Metall.*, 2000, **37**, (5), 276–288.
6. S. R. Koteswara Rao, G. Madhusudhan Reddy, P. Srinivasa Rao, M. Kamaraj and K. Prasad Rao: *Sci. Technol. Weld. Join.*, 2005, **10**, (4), 418–426.
7. G. Madhusudhan Reddy, A. A. Gokhale and K. Prasad Rao: *J. Mater. Sci.*, 1997, **32**, 4117–4126.
8. G. Madhusudhan Reddy, A. A. Gokhale and K. Prasad Rao: *Mater. Sci. Technol.*, 1998, **14**, (1), 61–63.
9. M. W. Brennecke: *Weld. J.*, Jan. 1965, 27s–39s.
10. J. P. Trail and D. W. Hood: *Weld. J.*, Sept. 1969, 395s–408s.
11. I. B. Robinson, F. R. Collins and J. D. Dowd: *Weld. J.*, May 1962, 221s–228s.
12. J. A. Hartman, R. J. Beil and G. T. Hahn: *Weld. J.*, Mar. 1987, 73s–83s.
13. V. D. Shelyagin, Y. Y. Khaskin, L. G. Shitova, T. N. Nabok, A. V. Siora, A. V. Bernatsky and T. G. Chizhskaya: *Paton Weld. J.*, 2005, **10**, 46–49.
14. G. Venkata Narayana, V. M. J. Sharma, V. Diwakar, K. Sree Kumar and R. C. Prasad: *Sci. Technol. Weld. Join.*, 2004, **9**, 121–130.
15. J. W. K. Van Boggeler, D. G. Eskin and L. Katgerman: *Scr. Mater.*, 2003, **49**, 712–722.
16. A. F. Norman, V. Drazhner and P. B. Prangnell: *Mater. Sci. Eng. A*, 1999, **A259**, 53–64.
17. V. Vaithyanathan, C. Wolverton and L. Q. Chen: *Acta Mater.*, 2004, **52**, 2973–2987.